Surface-Enhanced Raman Scattering from Functionalized Self-Assembled Monolayers. 2. Distance Dependence of Enhanced Raman Scattering from an Azobenzene Terminal Group

Qi Ye, Jianxin Fang,† and Li Sun*

Department of Chemistry, University of Minnesota, Minneapolis, Minnesota 55455

Received: March 10, 1997; In Final Form: June 2, 1997[⊗]

The distance dependence function (DDF) of surface-enhanced Raman scattering (SERS) has been measured. A novel feature of this work is that a self-assembled monolayer (SAM) of alkanethiol is used as the spacer layer whose length is varied from 1 to 15 methylene units. In addition, an azobenzene Raman label is covalently linked to the monolayer via an amide bond. Experimental DDF curves can be modeled reasonably with an electromagnetic (EM) field enhancement theory of Gersten and Nitzan. The characteristic distance at which SERS signals decrease by half is about 7 Å, 5 times shorter than previous values obtained with LB films as the spacer layer. We ascribe this discrepancy to the difference in the number of defects present in the spacer layer.

Introduction

Surface-enhanced Raman scattering (SERS) makes it possible to study structures and dynamics of molecules adsorbed on some metal surfaces, particularly on Cu, Ag, and Au surfaces.[1] Surface analytical techniques based on SERS share several unique advantages including submonolayer sensitivity, compatibility with aqueous environments, and relatively high molecular specificity. However, the potential of SERS has not been fully realized because of an incomplete understanding of the SERS enhancement mechanism. The slow progress in this area is largely due to the lack of experimental control over the parameters that dictate the magnitude of enhancement.

One such parameter is the distance between a Raman label and the substrate metal surface. Measuring the distance dependence function (DDF) has played an important role in elucidating the enhancement mechanism.[2] For example, electromagnetic (EM) field enhancement is a long-range effect, which would give a DDF of smaller decay rate than that resulted from a short-range chemical enhancement.[3]

Distance dependence study is also important to analytical applications of SERS.[4] For example, gold surfaces modified with self-assembled monolayers (SAMs) are being developed as a new type of chemical detector that promises enhanced selectivity and response time.[5] Obtaining an accurate and reliable DDF is certainly valuable for characterizing such detectors with SERS.

DDF has been measured previously by several groups of researchers with polymeric and LB films as the spacer layer.[2,6,7] However, the structural defects within these films probably have caused large errors in the corresponding DDFs. Indirect evidence for this possibility came from our early report in which a larger decay rate was observed when structurally ordered SAMs of alkanethiols were used as the spacer layer.[8]

In this work, we extend the above study by including more data points and using more reproducible Ag island films as the SERS substrate. We have chosen azobenzene as the Raman label because of its large scattering cross section,[9] (see Scheme 1). The covalent linkage between the azobenzene moiety and the alkanethiol spacer is important, since it ensures a consistent surface coverage and perhaps a uniform molecular orientation of the Raman label.

SCHEME 1

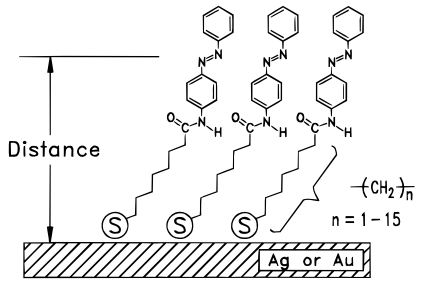

Experimental Section

Synthesis of *trans*-4-(*ω*-Mercaptoalkanamido)azobenzene (*t*-4MAZ). The synthesis of a series of alkanethiols with a pendent azobenzene group (*t*-4MAZ1 to *t*-4MAZ15), $HS(CH_2)_n$-CONHPhN═NPh (n = 1−5, 7, 11, 15) has been detailed in the Supporting Information. Briefly, an *ω*-bromoalkanoic acid was coupled to 4-aminoazobenzene, and the resulting bromide intermediate was then converted to the desired thiol.[8]

Sample Preparation and Measurements. Microscope cover slides (18 mm × 18 mm) were placed in a Teflon holder and cleaned by immersion in a 2% MICRO cleaner solution (Baxter International) for over 24 h. The slides were rinsed with a copious amount of water and then with absolute ethanol followed by drying under a flowing N_2 stream. Ag island films (150 Å mass thickness) on the slides were prepared by thermal evaporation from a resistively heated tungsten boat (charged with 99.999% Ag powder of 0.3−0.5 mm grain size, Johnson Matthey) at a 1 Å/s deposition rate under a base pressure of 6 × 10^{-6} Torr. Immediately after exposure to atmosphere, the island-coated slides were distributed and soaked in a series of 1.0 mM ethanolic thiol solutions for about 24 h. The slides were then rinsed with ethanol, dried with flowing N_2, and made ready for SERS measurements in air.

The Raman data acquisition system has been described previously.[10] Typical conditions for obtaining Raman spectra were 5.00 mW 647.1 nm excitation, 400 μm slit width (equivalent to 14 cm^{-1} band-pass), and 25 s effective integration time.

† Permanent address: Institute of Elemento-Organic Chemistry, Nankai University, Tianjin 300071, P.R.C.

* To whom correspondence should be addressed. Present address: Department of Chemistry, Texas A&M University, College Station, TX 77843-3255.

⊗ Abstract published in *Advance ACS Abstracts,* September 15, 1997.

S1089-5647(97)00869-9 CCC: $14.00

SCHEME 2

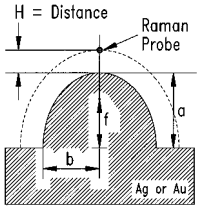

Data Analysis. A large relative error (50%) in SERS intensity was observed due to variations in island film morphology from batch to batch. However, using samples from the same batch of deposition reduced the error to 10%. Thus, a set of DDF data belonging to the same batch were first normalized to the first point in the set before being averaged with those belonging to other batches. To quantify peak intensity accurately, overlapping peaks were resolved through curve fitting (implemented with GRAMS/386, a spectral analysis software from Galactic Industries). Both peak area and peak height were used to estimate DDF, and no significant difference was found.

Experimental DDF data points were fitted with theoretical curves calculated according to an EM enhancement model developed by Gersten and Nitzan (GN model).[11] For a Raman probe located at a distance H from the tip of a hemispheroid protrusion on a perfectly conducting surface (Scheme 2), the enhancement factor K_{EF} for the probe is

$$K_{EF} \propto |A(a, b, H, \epsilon_L)A(a, b, H, \epsilon_S)|^2 \quad (1)$$

where $A(a, b, H, \epsilon_L)$ and $A(a, b, H, \epsilon_S)$ are the amplitude enhancement factors for the EM field at the excitation and the scattering wavelengths, respectively. These factors were evaluated according to the following equations:[7]

$$A(a, b, H, \epsilon_\lambda) = 1 + L(a, b, H)\frac{\epsilon_0 - \epsilon_\lambda}{\epsilon_\lambda - \epsilon_0 P(a, b, H)} \quad (2)$$

$$L(a, b, H) = \frac{\xi_0 Q_1'(\xi_1)}{Q_1(\xi_0)} \quad (3)$$

$$P(a, b, H) = \frac{\xi_0 Q_1'(\xi_0)}{Q_1(\xi_0)} \quad (4)$$

where $\xi_0 = a/f$, $\xi_1 = (a + H)/f$, $f = (a^2 - b^2)^{1/2}$, and a, b, and H are all geometric parameters of the model as illustrated in Scheme 2. Q_1 is a Legendre function of the second kind; and ϵ_0 and ϵ_λ denote dielectric constants of the ambient and the metal at a given wavelength λ,[12] respectively. The only adjustable parameters used in curve fitting were a and b, or equivalently, the size (a) and the shape (a/b) of the hemispheroid.

Results and Discussion

Figure 1 shows a set of representative spectra from SAMs of six azobenzene derivatives, each containing an odd number of methylene units. Most peaks above 900 cm^{-1} are due to the azobenzene moiety. For example, the peak at 993 cm^{-1} corresponds to the benzene ring breathing mode, 1137 cm^{-1} to the symmetric C—N stretching mode, and 1436 cm^{-1} to the N═N stretching mode. The peaks at 1459 and 1593 cm^{-1} correspond to benzene ring modes.[13]

The intensity dominance of azobenzene modes over modes from other parts of the molecule seems to suggest the presence of resonant enhancement in addition to SERS. To quantify the resonant contribution, we have measured the normal Raman scattering cross section of the 1436 cm^{-1} N═N stretching mode.[14] All *t*-4MAZs exhibit nearly identical cross sections in chloroform: i.e., 3.4×10^{-28} cm^2 sr^{-1}. This value is comparable to 1.0×10^{-28} cm^2 sr^{-1} for the normal Raman scattering cross section (the ethylene C═C stretching mode) of a structurally similar stilbene derivative under nonresonant excitation at 647 nm (ϵ_{max} = 25 000 cm^{-1} M^{-1} at 294 nm).[15] Therefore, resonant enhancement is not significant for *isolated t*-4MAZ molecules in chloroform, as one would expect based on their low molar extinction coefficient at 647 nm ($\epsilon_{647} = 0.7$ cm^{-1} M^{-1}, whereas $\epsilon_{max} = 240$ cm^{-1} M^{-1} at 445 nm).[15] It should be emphasized, however, that slight resonant enhancement is still possible for closely packed *t*-4MAZ molecules in a SAM because their optical absorption may be altered by intermolecular $\pi-\pi$ interactions.[9]

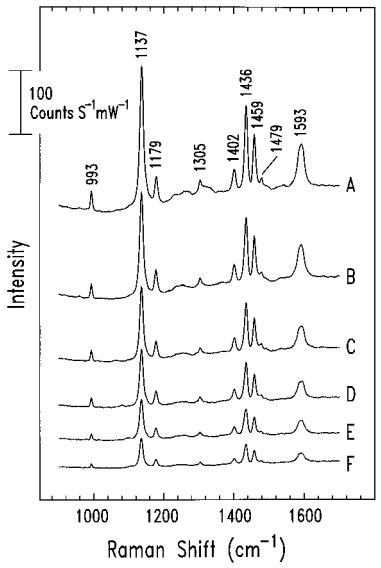

Figure 1. Representative spectra of SERS from SAMs of *t*-4MAZ, $HS(CH_2)_nCONHPhN{=}NPh$, on 150 Å thick Ag island films: (A) *t*-4MAZ1 or $n = 1$; (B) $n = 3$; (C) $n = 5$; (D) $n = 7$; (E) $n = 11$; (F) $n = 15$. The SERS enhancement factor for the 1137 cm^{-1} peak (symmetric C—N stretching mode) in (A) is about 3000.[14]

Figure 2 shows normalized experimental DDF points with a theoretical fit based on the GN model. The distance is estimated from the published thickness of an ω-mercaptoalkanoic acid SAM and the dimensions of an azobenzene molecule.[9,16] Since the azobenzene orientation is unknown, these estimates are certainly not accurate, although they are probably very precise. Another related problem is that different vibrational modes may be spatially localized at slightly different distances so that the corresponding DDF curves should not be plotted against the same distance axis. We have ignored this problem in Figure 2 because the shape of the decay curve is nearly exponential, thus insensitive to the location of the distance origin. Furthermore, the GN model also gives a nearly exponential fit.[11]

We have not included data points corresponding to spacers containing an even number of methylene units (*t*-4MAZ2 and *t*-4MAZ4) because these points lie outside the continuous trend shown in Figure 2. One possible explanation for this observation is that the orientation of the terminal azobenzene label depends on whether the number of methylene units is even or odd. The orientation, in turn, influences the observed SERS intensity,[17] resulting in a zigzagged decay curve. This "even-and-odd" effect has been observed in both SERS and surface IR spectra of *n*-alkanethiol SAMs with a terminal methyl group.[18]

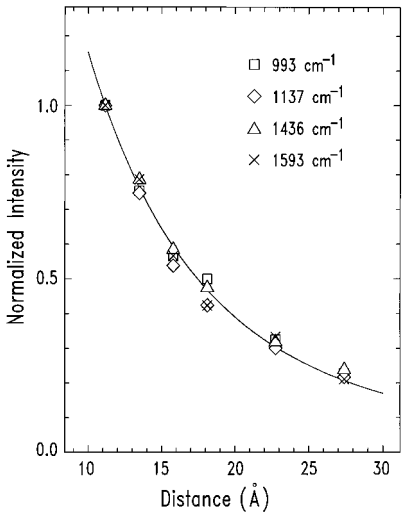

Figure 2. Normalized SERS enhancement factor as a function of distance. The six distance values correspond to the six SAMs of different methylene chain lengths. Symbols are experimental data, each type corresponding to a particular mode of vibration. The solid line is a good fit calculated according to the Gersten and Nitzan model with $a = 100$ nm and $b = 67$ nm. In comparison, the average width and height of Ag islands, as measured with a scanning force microscope, are 100 and 15 nm, respectively.

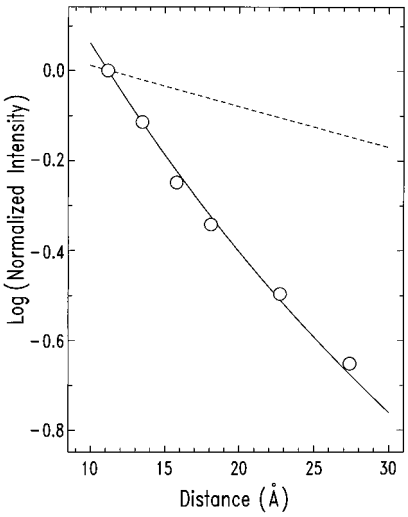

Figure 3. Comparison of SERS decay rates from different labs displayed in a semilogarithmic format. Circles are data points from this work, averaged over the four vibrational modes in Figure 2. The solid line represents a good fit using the GN model. The decay curves from both Cotton's and Kovacs's work are essentially the same in this distance range; they are shown as the dashed line.

Curve fitting of the experimental data according to the GN model gives us insight concerning the enhancement mechanism. The good fit shown in Figure 2 suggests that the decay could be due to a decreasing EM field.[19] Several factors, however, make it difficult to test the EM model more quantitatively. On the experimental side, Ag islands resemble an "island" or an oblate spheroid more than a prolate hemispheroid.[20,21] Thus, the hemispheroid model in Figure 2 that fits the experimental DDF is not a good representation of the actual island shapes, although the model does provide us with rough estimates for the size and the radius of curvature of those particles responsible for the observed SERS signal. Both the size and radius of curvature are difficult to define in a scanning-force-microscope image because of the irregular shape of Ag islands and distortion caused by a pyramidal scanning tip. In addition, Ag islands reside on a nonconducting glass surface instead of a conducting metal surface. On the theory side, the GN model ignores the extra intense EM field at the so-called "gap sites" between Ag islands. Recently, we have hypothesized that these sites contribute more to the enhancement factor than the sites on an isolated particle do.[10] Nevertheless, the simple GN model is rugged enough to still be useful. For instance, the shape of a calculated DDF curve depends strongly on the size and the shape of the protrusion but not much on the dielectric constant of the metal (e.g., errors due to the small particle limit) or on the particular type of the model (e.g., isolated spheroid vs hemispheroid on a plane).[11]

Within the experimental error, we do not observe any abrupt change in the decay rate along the DDF. Such a change would indicate that chemical enhancement is the dominant mechanism at short distances.[3] Weak chemical enhancement is expected because the π electrons on the azobenzene ring are relatively isolated from the free electrons in the metal even at a short spacer length. In other words, strong perturbation of adsorbate electronic structure associated with chemisorption, as observed by Campion,[22] is unlikely because the azobenzene π electrons are not directly conjugated with the chemical bonds immediately next to the chemisorption site. The lone pair electrons on the azo group may bond directly to surface Ag atoms, but this possibility is remote, since an Ag−azo bond is expected to be much weaker than an Ag−thiolate bond.

The nearly exponential decay of both experimental and theoretical DDF curves becomes more obvious in a semilogarithmic plot (Figure 3). The decay rate may be characterized by $d_{1/2}$, defined as the distance at which a SERS signal decays to half of its initial value. The $d_{1/2}$ from this work is about 0.7 nm, which is about 5 times smaller than the values derived from two independent studies led by Cotton and by Kovacs—both used LB films as the spacer.[6,7] Murray and Allara first measured the DDF of SERS with a poly(methyl methacrylate) spacer.[2] Interestingly, their $d_{1/2}$ of 1.5 ± 0.5 nm is closer to ours.

These apparent differences among decay rates from different labs can be caused by many factors, including substrate type, surface morphology, excitation wavelength, probe structure, and spacer structure. After comparing our experimental conditions with those used in Cotton's and Kovacs's work, we think that the defects within the spacer layer are an important factor that causes the aforementioned discrepancy. At defect sites, Raman labels are close to the substrate surface, which always leads to a SERS signal larger than expected. However, this increased signal is expected to cause a larger relative deviation at a larger spacer distance because the ideal signal intensity at such a distance is very small. Thus, as distance increases, the relative deviation (always positive) also increases. In other words, defects will lead to a decay rate smaller than that deduced from defect-free spacers. The smaller decay rates observed in the studies with LB film spacers are probably partly caused by defects. In addition, a more serious problem is the presence of defects larger than molecular dimensions. These defects would be produced when a LB film draped over the gap space between islands cracked,[7] producing an easy entry for Raman labels—especially those not covalently linked to the spacer layer. In contrast, a SAM spacer layer used here contains fewer defects[23−25] and covers all exposed island surface. This results in a larger decay rate, as we have observed, which is probably closer to the ideal, defect-free value.

Surface morphology (particle size, shape, and distribution) is another important factor that will influence the decay rate. In fact, this is what the GN model would predict through the a and b terms.[19] In a previous study,[8] the decay rate we measured on electrochemically roughened Ag electrodes is about twice

the rate obtained here on Ag island films. This is likely due to the difference in the average particle size of the above surfaces.[26]

Fabricating highly reproducible SERS-active morphology is still a challenge. Very often, two researchers or even the same researcher following exactly the same recipe for preparing Ag island films cannot produce two samples with exactly the same morphology or the same SERS response.[20] Slight variations in deposition conditions and trace amounts of contaminants in the vacuum chamber are the likely causes.[21,27] Fabricating particles with the desired size and shape is even more challenging. Recently, techniques for fabricating and characterizing better-defined SERS-active particles have been reported.[10,28] If these techniques can be refined to improve their reproducibility, they will allow us to have a more quantitative comparison between measured decay rates and those predicted from theories.

Conclusions

Two major conclusions can be drawn. First, SERS decays as a function of distance about 5 times faster than previously thought. The characteristic distance at which SERS signals decrease by half is about 7 Å. The experimental decay curves can be modeled by the EM theory of Gersten and Nitzan. In addition, the lack of abrupt changes along a decay curve implies that chemical enhancement is not the dominant mechanism even at the shortest spacer distance used in this work. Second, the defect sites within a spacer layer greatly influence the decay rate. The more defects there are, the slower the SERS signal decays.

Finally, we believe that surface morphology is another important yet unevaluated factor that dictates the decay rate. Although relatively reproducible, the Ag island films used here are by no means a "well-defined" SERS substrate that is amenable to direct comparison with EM enhancement models.

Acknowledgment. L.S. gratefully acknowledges financial support from National Science Foundation (CHE-9531243). J.F. acknowledges an IRSEP scholarship sponsored by Nankai University and University of Minnesota.

Supporting Information Available: Synthesis of the azobenzene-terminated self-assembling molecules and electrochemical characterization of the resulting SAMs (14 pages). Ordering information is given on any current masthead page.

References and Notes

(1) (a) Birke, R. L.; Lu, T.; Lombardi, J. R. In *Techniques for Characterization of Electrodes and Electrochemical Processes*; Varma, R., Shelman, J. R., Eds.; Wiley: New York, 1991. (b) Moskovits, M. *Rev. Mod. Phys.* **1985**, *57*, 783.

(2) (a) Murray, C. A.; Allara, D. L.; Rhinewine, M. *Phys. Rev. Lett.* **1981**, *46*, 57−60. (b) Murray, C. A.; Allara, D. L. *J. Chem. Phys.* **1982**, *76*, 1290−1303.

(3) Otto, A. *J. Raman Spectrosc.* **1991**, *22*, 743−752.

(4) (a) Cotton, T. M.; Kim, J.-H.; Chumanov, G. D. *J. Raman Spectrosc.* **1991**, *22*, 729−742. (b) Garrell, R. L. *Anal. Chem.* **1989**, *61*, 402A−411A. (c) Zhang, W.; Vivoni, A.; Lombardi, J. R.; Birke, R. L. *J. Phys. Chem.* **1995**, *99*, 12846−12857. (d) Macdonald, I. D. G.; Smith, W. E. *Langmuir* **1996**, *12*, 706−713. (e) Ford, J. F.; Vickers, T. J.; Mann, C. K.; Schlenoff, J. B. *Langmuir* **1996**, *12*, 1944−1946.

(5) (a) Carron, K.; Peltersen, L.; Lewis, M. *Environ. Sci. Technol.* **1992**, *26*, 1950−1954. (b) Thompson, W. R.; Pemberton, J. E. *Anal. Chem.* **1994**, *66*, 3362−3370. (c) Crooks, R. M.; Chailapakul, O.; Ross, C. B.; Sun, L.; Schoer, J. K. In *Chemically Sensitive Interfaces*; Mallouk, T. E., Harrison, D. J., Eds; ACS Symposium Series; American Chemical Society: Washington, DC, 1993. (d) Häussling, L.; Ringsdorf, H.; Schmitt, F.-J.; Knoll, W. *Langmuir* **1991**, *7*, 1837−1840. (e) Prime, K. L.; Whitesides, G. M. *Science* **1991**, *252*, 1164−1167.

(6) Cotton, T. M.; Uphaus, R. A.; Mobius, D. *J. Phys. Chem.* **1986**, *90*, 6071−6073.

(7) Kovacs, G. J.; Loutfy, R. O.; Vincett, P. S.; Jennings, C.; Aroca, R. *Langmuir* **1986**, *2*, 689−694.

(8) Tsen, M.; Sun, L. *Anal. Chim. Acta* **1995**, *307*, 333−340.

(9) (a) Caldwell, W. B.; Chen, K.; Herr, B. R.; Mirkin, C. A.; Hulteen, J. C.; Van Duyne, R. P. *Langmuir* **1994**, *10*, 4109−4115. (b) Caldwell, W. B.; Campbell, D. J.; Chen, K.; Herr, B. R.; Mirkin, C. A.; Malik, A.; Durbin, M. K.; Dutta, P.; Huang, K. G. *J. Am. Chem. Soc.* **1995**, *117*, 6071−6082.

(10) Xiao, T.; Ye, Q.; Sun, L. *J. Phys. Chem. B* **1997**, *101*, 632.

(11) Gersten, J. I.; Nitzan, A. *J. Chem. Phys.* **1980**, *73*, 3023.

(12) Johnson, P. B.; Christy, R. W. *Phys. Rev. B* **1972**, *6*, 4370.

(13) (a) Lin-Vien, D.; Colthup, N. B.; Fateley, W. G.; Grasselli, J. G. *The Handbook of Infrared and Raman Characteristic Frequencies of Organic Molecules*; Academic Press: San Diego, 1991; p 198. (b) Trotter, P. J. *Appl. Spectrosc.* **1977**, *30*, 30−35. (c) Hacker, H. *Spectrochim. Acta* **1965**, *21*, 1989.

(14) The normal and surface Raman scattering cross sections were measured according to the method in ref 10.

(15) The molar absorption coefficients were either measured in our lab or found in the literature. For example, see the following. Hirayama, K. *Handbook of Ultraviolet and Visible Absorption Spectra of Organic Compounds*; Plenum Press: New York, 1967.

(16) Bain, C. D.; Troughton, E. B.; Tao, Y.-T.; Evall, J.; Whitesides, G. M.; Nuzzo, R. G. *J. Am. Chem. Soc.* **1989**, *111*, 321−335.

(17) (a) Creighton, J. A. In *Spectroscopy of Surfaces*; Clark, R. J. H., Hester, R. E., Eds.; Wiley: New York, 1988. (b) Carron, K. T.; Hurley, L. G. *J. Phys. Chem.* **1991**, *95*, 9979.

(18) (a) Walczak, M. M.; Chung, C.; Stole, S. M.; Widrig, C. A.; Porter, M. D. *J. Am. Chem. Soc.* **1991**, *113*, 2370−2378. (b) Bryant, M. A.; Pemberton, J. E. *J. Am. Chem. Soc.* **1991**, *113*, 8284−8293.

(19) The decay rate as predicted by the GN model decreases as the aspect ratio increases or as the overall size decreases. Consequently, there exist more than one set of aspect ratio and size combinations, all leading to a good fit. The parameters in Figure 2 were selected by considering the measured island sizes and a plausible aspect ratio.

(20) (a) Van Duyne, R. P.; Hulteen, J. C.; Treichel, D. A. *J. Chem. Phys.* **1993**, *99*, 2101−2115. (b) Schlegel, V. L.; Cotton, T. M. *Anal. Chem.* **1991**, *63*, 241.

(21) (a) Semin, D. J.; Rowlen, K. L. *Anal. Chem.* **1994**, *66*, 4324. (b) Roark, S. E.; Rowlen, K. L. *Anal. Chem.* **1994**, *66*, 261.

(22) Campion, A.; Ivanecky, J. E., III; Child, C. M.; Foster, M. *J. Am. Chem. Soc.* **1995**, *117*, 11807−11808.

(23) Many studies have shown that SAMs are structurally more ordered than LB films. For early reviews, see the following. (a) Swalen, J. D.; Allara, D. L.; Andrade, J. D.; Chandross, E. A.; Garoff, S.; Isreaelachvili, J.; McCarthy, T. J.; Murray, R.; Pease, R. F.; Rabolt, J. F.; Wynne, K. J.; Yu, H. *Langmuir* **1987**, *3*, 932−950. (b) Ulman, A. *An Introduction to Ultrathin Organic Films: From Langmuir-Blodgett to Self-Assembly*; Academic Press: Boston, 1991. (c) Dubois, L. H.; Nuzzo, R. G. *Annu. Rev. Phys. Chem.* **1992**, *43*, 437−463.

(24) A recent report has shown that even SAMs covering small metal clusters of 2.4 nm diameter can act as good spacers for modulating the electron hopping between metal clusters. Terrill, R. H.; Postlethwaite, T. A.; Chen, C.-H.; Poon, C.-D.; Terzis, A.; Chen, A.; Hutchison, J. E.; Clark, M. R.; Wignall, G.; Londono, J. D.; Superfine, R.; Falvo, M.; Johnson, C. S., Jr.; Samulski, E. T.; Murray, R. W. *J. Am. Chem. Soc.* **1995**, *117*, 12537−12548.

(25) We are not aware of any convenient method for quantifying the defects within a SAM on Ag islands. Instead, we have studied defects within *t*-4MAZ SAMs on Au electrodes. Our results show that the defect density for a *t*-4MAZ SAM is low and comparable to that for a well-ordered SAM of *n*-alkanethiol containing the same number of methylene units. See Supporting Information for details.

(26) Sun, L. Ph.D. Thesis, Northwestern University, Evanston, IL, 1990.

(27) (a) Damodara Das, V.; Murali Sastry M. S. *J. Appl. Phys.* **1986**, *59*, 3184. (b) Andersson, T.; Granqvist, C. G. *J. Appl. Phys.* **1977**, *48*, 1673.

(28) (a) Freeman, R. G.; Grabar, K. C.; Allison, K. J.; Bright, R. M.; Davis, J. A.; Guthrie, A. P.; Hommer, M. B.; Jackson, M. A.; Smith, P. C.; Walter, D. G.; Natan, M. J. *Science* **1995**, *267*, 1629−1632. (b) Li, W.; Virtanen, J. A.; Penner, R. M. *J. Phys. Chem.* **1994**, *98*, 11751. (c) Nie, S.; Emory, S. R. *Science* **1997**, *275*, 1102−1106.